MODELLING OF CFRP STRENGTHENING ON THE BEHAVIOR OF RC SLENDER COLUMNS

Le Nguyen Khuong[1]*

Abstract: *This paper addresses the strength and deformation capacity of slender columns retrofitted by externally bonded Carbon Fiber-Reinforced Polymers (CFRP) subjected to seismic loading. The behaviour of RC columns depending on the CFRP confinement (carbon CFRP jacket) and on flexural reinforcement (carbon plates) was analysed by a nonlinear finite element method based on multilayer shell element and multifiber beams with plasticity and damage models. The numerical results in terms of the load-displacements are very consistent with experimental data. The observed failure modes and crack patterns are satisfactorily reproduced for both columns, without or with the CFRP strength.*

Keywords: *FEA, concrete columns, retrofitting, CFRP.*

Received: October 9th, 2017; revised: October 30th, 2017; accepted: November 2nd, 2017

1. Introduction

Considering that the major cause of construction collapse is column failure, specific retrofitting techniques and design rules have to be established. In this context, the use of Fibre Reinforced Polymer (CFRP) has significantly increased in construction and civil engineering fields. Indeed, bonding of external CFRP reinforcements is now recognized as an effective technique for the strengthening of reinforced concrete (RC) structures, and it can be particularly useful for seismic retrofitting. Most studies conducted to date on reinforcement of existing RC columns using externally bonded CFRP have mainly been focused on confinement efficiency [1-3] and strengthening [4-6]. However, few experimental data are currently available regarding the behavior of reinforced concrete columns reinforced by associating a flexural strengthening, achieved by CFRP plates bonded longitudinally, with a confinement by wrapping.

In this context, an experimental campaign in actual large scale reinforced concrete columns with different reinforcement configurations was completed and tested in the laboratory structures IFSTTAR located in Paris by [7] in the INPERMISE project. Its objective was to compare and quantify the specific contribution of each process, namely the action of CFRP confinement, the action of strips CFRP to bending, the action of the anchoring of these strips and the combination of these reinforcement methods. The experimental results were analysed by simple formulas to estimate the maximum strength of each column but the ductility and the significant drop in resistance when breaking the anchor are not reproduced. In this paper, numerical analysis by using different modeling technique will be used to reproduce the later behaviors of each column.

2. RC columns retrofitted by CFRP

A total of 8 representative scale RC column specimens were constructed. Specimens consisted of $0.25\times0.37\times2.50m^3$ columns connected to $1.25\times1.00\times1.00m^3$ RC stubs (Fig. 1). Six 10mm steel deformed rebars were used for longitudinal reinforcement and 6mm ties spaced at 150mm, were used for transverse reinforcement. For the 8 columns, four CFRP strengthening configurations were studied so: Without strengthening (reference specimens PRef1 and PRef2); confinement specimens PC1 and PC2 (8 strips CFRP dimension 300×1440 mm^2); a combination of confinement and laminates for specimens PCL1 and PCL2 (10 lamellas of dimension 50×2500 mm^2 and 8 strips CFRP dimension 300×1440 mm^2); and a combination of confinement and anchored laminates (PCLA1 and PCLA2) (10 lamellas of dimension 50×2500 mm^2, 8 strips CFRP dimension $300\times1440mm^2$ and anchoring system on the large face). Those strengthen-

[1] Dr, University of Transport Technology.
** Corresponding author. E-mail: khuongln@utt.edu.vn.*

ing configurations are summarized in (Fig. 2). Repeating the experiments twice was an experimental choice to increase the confidence level in the results.

These design details produce a longitudinal reinforcement ratio of 0.5%. Reinforcement bars showed yield stress and ultimate strength of 500 MPa and 610 MPa respectively. The column was considered to have reached its ultimate condition when the specimen is unable to sustain an applied lateral load inferior to 50% of the maximum lateral capacity observed during the test.

The compression strength of concrete at 28 days was evaluated at 41.5 MPa. The wetlay up process was used for the CFRP confining jacket. Saturated carbon fibre sheets were wrapped around the column while flexural reinforcement was achieved by bonding pultruded CFRP plates. Characteristics of CFRP reinforcements are summarized in Table 1 presented characteristics are those reported by the manufacturer.

Table 1. *Manufacturer reported CFRP reinforcement (Freyssinet products)*

Properties	CFRP sheets (TFC©)	Pultruded plates
Tensile modulus (MPa)	105 000 MPa	160 000MPa
Ultimate strain (%)	1.1	0.7
Thickness	0.48 mm	1.2 mm
Width	300 mm	50 mm

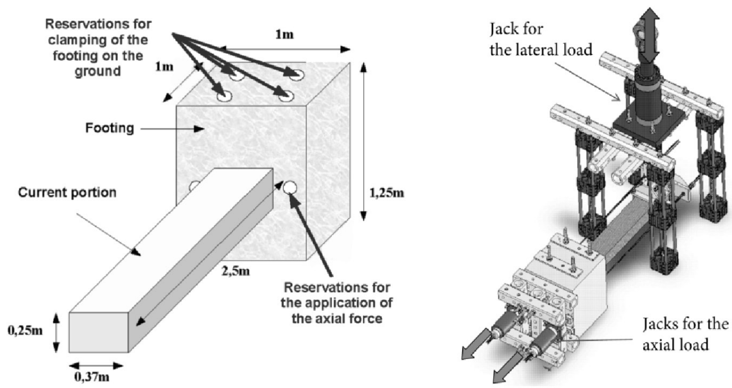

Figure 1. *Column dimensions and test setup [7]*

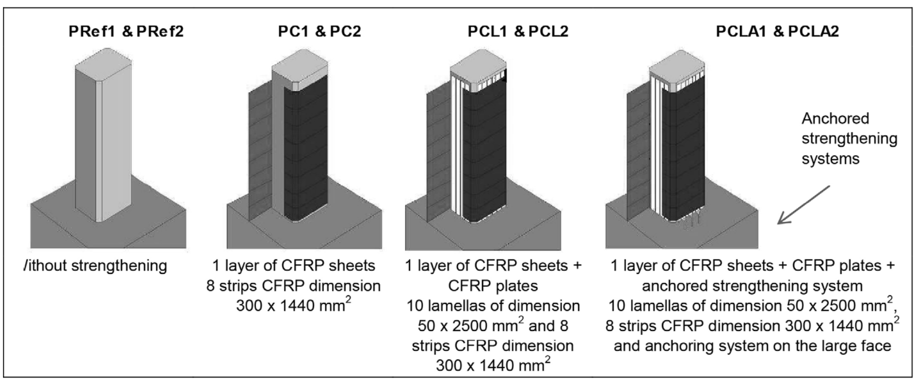

Figure 2. *CFRP strengthening configuration [7]*

Seismic load was simulated by applying cyclic lateral displacements gradually increasing (representative of a seismic loading), while the column was simultaneously subjected to a constant axial load (simulating gravity load). The constant axial load of 700kN was applied through a pair of hydraulic jacks linked to prestressing tendons, and displacement controlled lateral load was applied thanks to another hydraulic (Fig. 1). After the application of the axial load, the specimen was subjected to progressively increasing lateral displacement cycles. Two fully reversed cycles were applied for each displacement step. Those displacement steps, referred here as “drift ratio”, were defined as a ratio of the column height: 0.25%; 0.5%; 1%; 2%; 4%; etc. until failure. The column was considered to have reached its ultimate condition when the specimen is unable to sustain an applied lateral load inferior to 50% of the maximum lateral capacity observed during the test.

3. Modelling of CFRP strengthening

The current work deals to valid two different frame element formulations, namely the multifiber beam element and the multilayer shell element using the finite element code CAST3M [8] in order to compare with the experimental results. The numerical model was developed with the same geometrical and loading characteristics previously presented.

For the multifiber beam element approach, the uniaxial behavior of concrete was adopted for describing the nonlinear behavior of the fiber type beam elements. The uniaxial behavior of concrete was adopted for describing the nonlinear behavior of the fiber type beam elements [9].

For the multilayer shell element, an elasto-plastic concrete model that provides acceptable representation of the cyclic inelastic behavior of reinforced concrete under cyclic loading was used. This model Merabet & Reynouard [10], adopts the concept of a smeared crack approach with a possible double cracking only at 90°. It is based upon the plasticity theory for uncracked concrete with isotropic hardening and associated flow rule. Two distinct criteria describe the failure surface: Nadai in compression and bi-compression and Rankine in tension. Hardening is isotropic and an associated flow rule is used. When the ultimate surface is reached in tension, a crack is created perpendicularly to the principal direction of maximum tensile stress, and its orientation is considered as fixed subsequently. Each direction is then processed independently by a cyclic uniaxial law, and the stress tensor in the local co-ordinate system defined by the direction of the cracks is completed by the shear stress, elastically calculated with a reduced shear modulus modulus, to account for the effect of interface shear transfer. The model has been described in detail and verified elsewhere [11-12].

For steel, a cyclic model that can take into account the Bauschinger effect and buckling of reinforcing bars has been adopted. The cyclic behavior is described by the formulation proposed by Giuffré and Pinto and implemented by [13].

The behavior of reinforced concrete structures retrofitting by the CFRP bonding technique outside the section, in the form of thin plates or sheets, is often dominated by three effects: the debonding between CFRP and concrete; the bend strength of CFRP stirrups and the behavior and effectiveness of CFRP wrap in the confinement.

It's important to note that the specimens have characteristics of the old constructions, not submitted to the general principles of seismic design. Therefore, the confinement effect of the horizontal reinforcement is not considered in the concrete model.

3.1 Debonding Behavior

Despite the extensive research that has been carried out, there are still significant uncertainties and difficulties in finite element modeling of CFRP detachment due to the complex behavior of cracked concrete. In general, there are two approaches to simulate this type of ruin. The first is to introduce interface elements between the CFRP and concrete [14], and the ruin corresponding to the breakdown of these elements. The success of this approach depends on the behavior law specified for the interface elements but in general the numerical scheme presents difficulties of convergence. Concerning the second approach, the use of interface elements is avoided, and the debonding is directly simulated by the modeling of the cracking of the concrete adjacent to the adhesive layer. [15] proposed an approach of this type: the carbon fiber elements are directly connected to concrete elements that make up the adjacent concrete, taking concrete element sizes well below the physical thickness of the layer of concrete that loosens (of the order of a few mm). This method makes it possible to translate correctly the behavior of the detachment without problem of numerical convergence but the resolution becomes very heavy in the practical cases where the number of elements is important.

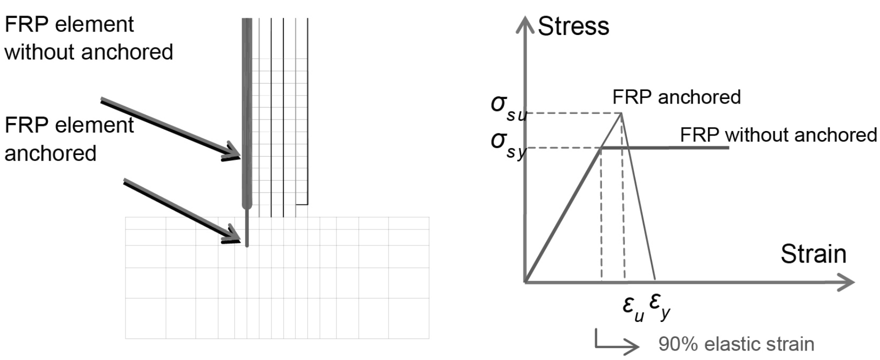

***Figure 3.** Modeling of CFRP stirrups*

For the prediction of the debonding, the use of a coefficient of efficiency of the CFRP is necessary. This coefficient depends on the configuration of the reinforcements. It has been the subject of several research studies have been carried out [16]. In the case of non-anchored reinforcements, this value is equal to the elastic strength of the CFRP multiplied by the efficiency coefficient of 0.9, whereas for the anchorages it is considered the elastic strength of the CFRP. In order to reproduce the observed debonding while accounting for the tensile force in the CFRP strips due to the anchorage, an elastoplastic model has been proposed (Figure 3). This approach permits to avoid the introduction of an interface element between the concrete and the CFRP strips and turns out to be efficient for modeling the CFRP-retrofitted RC slender column.

3.2 Bend strength of CFRP stirrups

In the case of reinforcement with respect to the bending, the CFRP is oriented axially (parallel to the axis of the element). The presence of the CFRP on one or more faces of an element plays a role similar to that of additional longitudinal reinforcements. The modeling strategy adopted therefore consists in representing the reinforcement by additional layers in the section of the multilayer element and of the additional fibers within the section of the multi-fiber beam element. The section of the element is then composed of layers or fibers of concrete, steel and CFRP (Fig. 4). This modeling technique does not present any significant difficulties and can therefore be simply integrated into a finite element code without excessively adding to the calculation process.

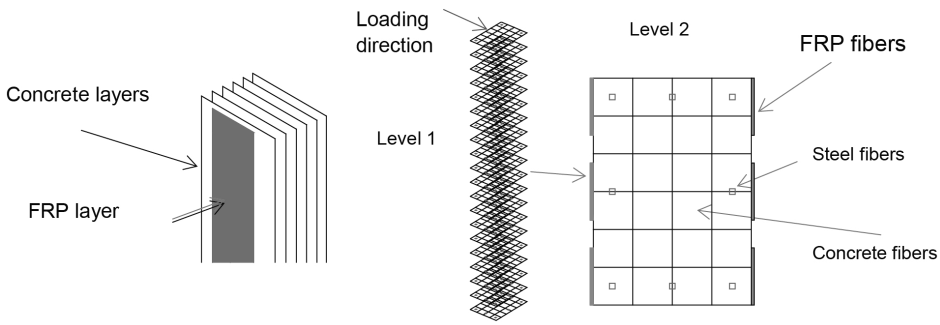

Figure 4. *CFRPs in the multi-layer shell element (left) and the multi-fiber beam element (right)*

3.3 Effectiveness of CFRP wrap in the confinement

Over the last three decades, the behavior of confined concrete has been extensively studied by many researchers, and the main mechanisms behind the containment are now well known and established. Despite extensive research, an analytical tool suitable for predicting the behavior of CFRP confined concrete has not yet been established for the diversity of reinforcement configurations. Most of the available models are empirical in nature and have been calibrated to available experimental data. In the first category, compressive strength, ultimate axial strain and stress-strain behavior of CFRP confined concrete are predicted using analytical equations based directly on the interpretation of the experimental results. In the second category, stress-strain curves of confined concrete are generated using an incremental numerical procedure. In this second approach, an active confinement model is used to evaluate the axial stress and the stress of the concrete, passively confined under a given confinement pressure. In this context, the interaction between the concrete and the confinement material is clearly represented by the equilibrium of forces considering the compatibility of the radial displacement.

In order to reflect the effect of confinement, the concrete behavior law must be modified in order to take into account the following modifications: tensile and compressive strength, post-peak tensile slopes and compression by modifying the concrete failure energy due to the presence of the CFRPs, the cyclic opening and reclosing laws of cracks. In this work, the principle of modeling the behavior of confined concrete is similar. The compression failure strain are summarized in the study by [17]. For this work, the compressive strength and failure strain adopted by Eurocode 8 [18] has been used:

$$f_{cc} = f_c + \psi_f \cdot k_1 \cdot k_c \cdot k_h \cdot f_{pu,k} \tag{1}$$

$$\varepsilon_{cc} = \varepsilon_{c0}\left[1+5\left(\frac{f_{cc}}{f_{c0}}-1\right)\right] \tag{2}$$

The unconfined concrete strain (εc0) corresponding to the maximum compression strength was taken as 0.003 while the value for the confinement factor was 1.16 for the confined concrete and 1.0 for the concrete cover. The modeling parameters for the columns are presented in the Table 2.

Table 2. *Numeric parameter for the columns*

	Definition	PRef	PC	PCL	PCLA
E_0	Young Modulus [GPa]	28.0	28.0	28.0	28.0
f_c	Compressive strength [MPa]	40.0	45.0	45.0	45.0
f_t	Tensile strength [MPa]	3.2	3.6	3.6	3.6
ε_{tm}	Cracking strain	4.5E-03	4.5E-3	5.5E-3	5.5E-3
ε_{rupt}	Fracture strain in compression	20.0E-03	45.0E-3	50.0E-3	50.0E-3

4. Comparison between experimental and numerical results

The load-lateral displacements envelope curves of Pref, PC, PCL and PCLA are presented in Figs. 5 and 6. Concerning the resistance to lateral force, it can be observed that the load maximum recovery by the specimen reference (Pref) is essentially identical to that given by the retrofitting specimens (PC and PCL). If the composite strengthening often has demonstrated a performance in terms of increasing the support capacity of the column, even in the case of the composed flexure [19-20], retrofitting configurations tested on PC and PCL (respectively confinement and confinement coupled to the laminate single) does not allow to take a larger lateral force, even when it is accompanied by a confinement reinforcement bending (PCL). The configuration combining the confinement and the laminate anchored to the bending (PCLA) provide a net increase of the maximum lateral resumed (37% compared to the force absorbed by PCL).

Concerning the ductility behavior, the ultimate lateral displacement of specimens retrofitted is about twice this once of reference specimen. Indeed, the composite confines the compressed concrete, including the plastic hinge, will delay the damage and limit the crack width, both in the tension part and compressed part. Overall, the confinement allows delay breaking capacity and to increase the lateral displacement of the columns, making them more efficient.

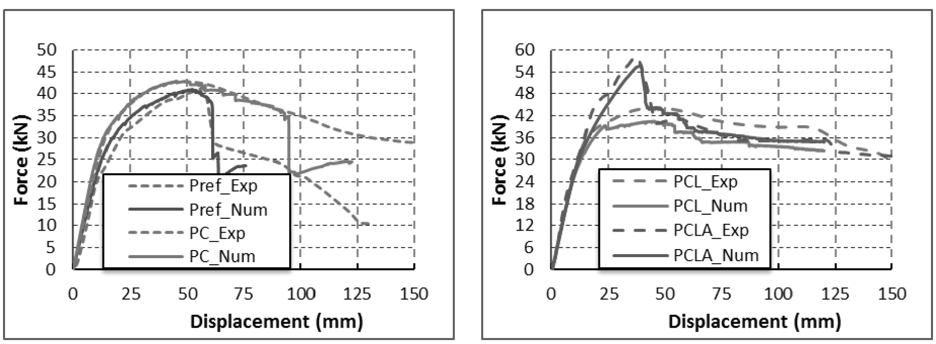

(a) (b)

Figure 5. *Multilayer shell element (*_Num: numeric result; *_Exp: Experimental result)*

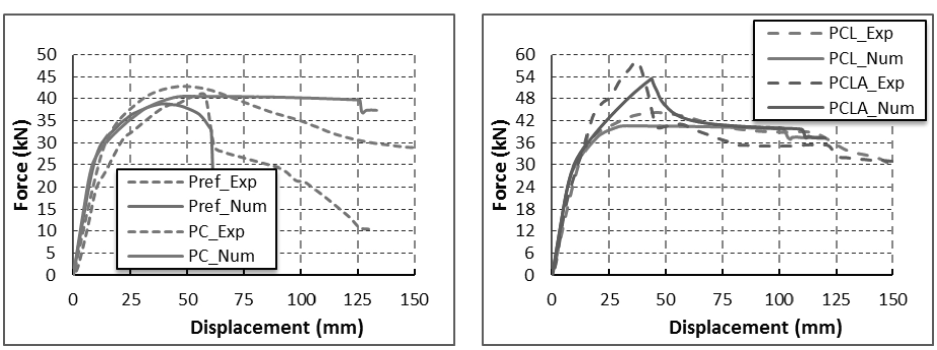

Figure 6. *Multifiber beam element (*_Num: numeric result; *_Exp: Experimental result)*

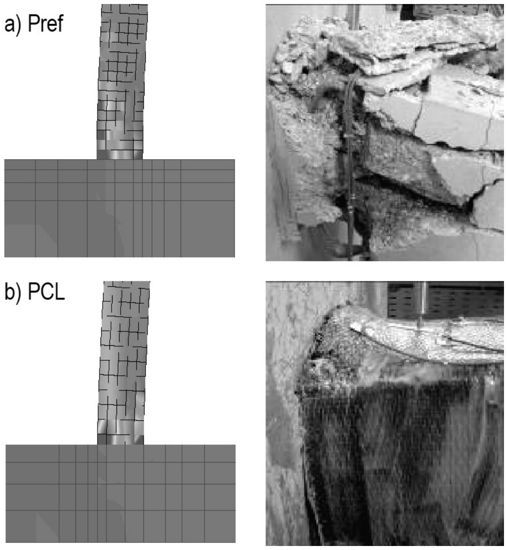

Figure 7. Cracking patterns corresponding to the displacement of 50mm by multilayer element approach and cracking pattern in end column after testing

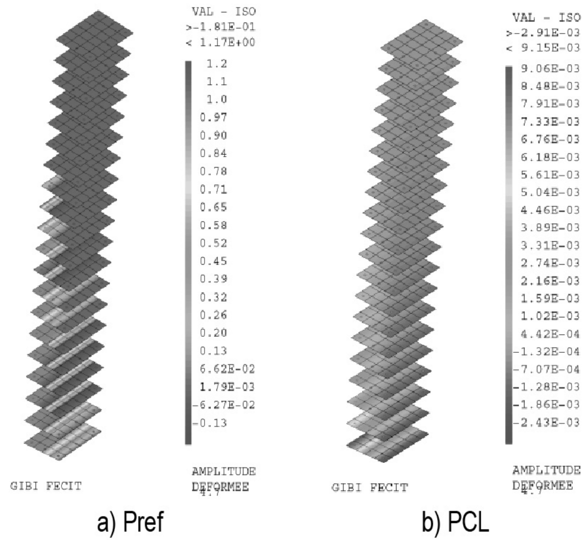

Figure 8. Cracking patterns corresponding to the displacement of 50mm by multifiber element approach

The two numerical pushover curves are very close to the experimental data, with a slight overestimation of the strength. In particular, the loss of sudden resistance of the PCLA specimen is due to the rupture of the anchored CFRP bands. In addition to the load–displacement curves, the failure modes predicted by the numerical approaches are confronted with the observed failure modes in pushover tests.

If we compare the cracking patterns predicted by numerical calculation, we can see that the cracks are more distributed in the case of the reference column without strengthning (Pref) and more concentrated towards the critical section in the case of strengthning. In order to investigate the confinement effect, the damage pattern corresponding to a 50 mm displacement of the Pref and PCL are shown in Figs. 7 and 8. For the Pref column, the cracks develop first in the critical section between the current part of the column and the foundation, and then they propagate over the column height. For the reinforced columns, the damage area remains more localized at the bottom of the column.

5. Conclusion

In this paper, the CFRP strengthening on the behavior of RC slender columns were simulated by different modeling techniques. Consideration of confinement and flexural reinforcement was also discussed. CFRP reinforcement is taken into account by modifying the parameters of concrete behavior laws, such as tensile and compressive strengths and softening slopes by modifying the failure energies. The CFRP bending reinforcement strips without anchoring were modeled by bar elements having a resilient behavior up to 90% of the CFRP strength, while the anchored CFRP strips have an elastic behavior up to the resistance of the CFRP. A nonlinear finite element method is used, based on multilayer shell element and multifiber beams with plasticity and damage models. The pushover curves and the ruin modes found are very consistent with the experimental results. In this study, we validated the approaches and assumptions adopted in order to correctly predict the behavior of reinforced structural elements. This is a first step before dealing with the case of complete structures.

References

1. Chaallal O., Shahawy M. (2000), “Performance of Fiber-Reinforced Polymer-Wrapped Reinforced Concrete Column under Combined Axial-Flexural Loading”, *American Concrete Institute Structural Journal*, 97(4):659-668.

2. Li J., Hadi M.N.S. (2003), “Behaviour of externally confined high-strength concrete columns under eccentric loading”, *Composite Structures Journal*, 62(2):145-153.

3. Quiertant M., Clement J.L. (2011), “Behavior of RC columns strengthened with different CFRP systems under eccentric loading”, *Construction and Building Materials*, 25(2):452-460.

4. Chen J.F., Teng J.G. (2003), “Shear capacity of FRP-strengthened RC beams: FRP debonding”, *Construction and Building Materials*, 17(1):27-41.

5. Colomb F., Tobbi H., Ferrier E., et al. (2008), “Seismic retrofit of reinforced concrete short columns by CFRP materials”, *Composite Structures Journal*, 82(4):475-487.

6. Sause R., Harries K., Walkup S., et al. (2004), “Flexural Behavior of Concrete Columns Retrofitted with Carbon Fiber-Reinforced Polymer Jackets”, *American Concrete Institute Structural Journal*, 101(5):708-716.

7. Sadone R., Quiertant M., Mercier J., et al. (2012), “Experimental study on RC columns retrofitted by FRP and subjected to seismic loading”, *6th International Conference on FRP Composites in Civil Engineering CICE 2012*, Rome, 157-169.

8. Le Fichoux E. (2011), *Presentation Et Utilisation De Cast3m*, Support of CEA (http://www-cast3m.cea.fr)

9. Guedes J., Pegon P., Pinto A. (1994), *A fibre timoshenko beam element in castem2000*, Special publication Nr. I.94.31, J.R.C., I-21020, Joint Research Center. Ispra, Italy.

10. Merabet O., Reynouard J. (1999), “Formulatin d’un modèle élasto-plastique fissurable pour le béton sous chargements cycliques”, *Contrat de recherche avec EDF*.

11. Ile N., Reynouard J. (2000), “Nonlinear analysis of reinforced concrete shear wall under Earthquake loading”, *Journal of Earthquake Engineering*, 4(2):183-213.

12. Khuong L. K., Brun M., Limam A., et al. (2014), “Pushover experiment and numerical analyses on CFRP-retrofit concrete shear walls with different aspect ratios”, *Composite Structures Journal,* Volume 113:403-418.

13. Menegotto M., Pinto P. (1973), “Method of analysis for cyclically loaded reinforced concrete plane frames including changes in geometry and non-elastic behaviour of elements under combined normal force and bending”, *International Association of Bridge and Structural Engineering*, Libson, Portugal, 13:15-22.

14. Ferracuti B., Savoia M., Mazzotti C. (2007), “Interface law for FRP-concrete delamination”, *Composite Structures Journal,* 80(4):523-531.

15. Lu X.Z., Teng J.G., Ye L.P., et al. (2005), “Meso-scale finite-element model for FRP sheets/plates externally bonded to concrete”, *Engineering Structures*, 27(4):564-575.

16. Barbato M. (2009), “Efficient finite element modelling of reinforced concrete beams retrofitted with fibre reinforced polymers”, *Computers & Structures Journal*, 87(3-4):167-176.

17. De Lorenzis L., Tepfers R. (2003), “Comparative Study of Models on Confinement of Concrete Cylinders with Fiber-Reinforced Polymer Composites”, *Journal of Composites for Construction*, 7(3):219-237.

18. EN 1998-3 (2005), *Eurocode 8: Design of structures for earthquake resistance - Part 3: Assessment and retrofitting of buildings*.

19. Roy N., Labossière P., Proulx J., et al. (2009), “FRP Wrapping of RC Structures Submitted to Seismic Loads”, *Seismic Risk Assessment and Retrofitting*, Springer Netherlands, 297-305.

20. Iacobucci R., Sheikh S. (2003), “Retrofit of Square Concrete Columns with Carbon Fiber-Reinforced Polymer for Seismic Resistance”, *American Concrete Institute Structural Journal*, 100(6):785-794.